^{3}He Impurity States on Liquid ^{4}He: From Thin Films to the Bulk Surface

N. Pavloff and J. Treiner

Division de Physique Théorique, Institut de Physique Nucléaire, Orsay, France*

The structure of the states accessible to ^{3}He impurities in films of liquid ^{4}He on Nuclepore is investigated using a density functional approach with a finite-range effective interaction. In thick films, one finds that the two lowest states are localized in the surface region. For thinner films, the variation with film thickness of the first three states results from a delicate balance between the attractive tail of the substrate potential and the quantum finite-size effect. The existence of states localized in the second layer of the films is discussed. The energy difference between the ground state and the first excited state agrees with the recent determination of Higley, Sprague, and Hallock from magnetization measurements. The effective mass of the ground state has a structure similar to that obtained by Krotscheck and coworkers and exhibits a maximum for a ^{4}He coverage of 0.15 $\mathring{A}^{-2}$, in agreement with the data of Gasparini and coworkers. A similar behavior is predicted for the effective mass of the first, second, and third excited states. The structure of the energy spectrum may also explain former results on third-sound measurements in thin mixture films by Laheurte et al. and by Hallock.

1. INTRODUCTION

Much experimental and theoretical work has been devoted to the study of ^{3}He impurities on liquid ^{4}He. As originally proposed by Andreev,[1] ^{3}He impurities in the bulk liquid are localized on the surface, and in a series of beautiful experiments, Edwards and coworkers[2] have confirmed the behavior of a two-dimensional Fermi gas (2DFG), built on a ground state with energy -5 K and characterized by an effective mass in the range 1.30–1.45 times

---

the free mass. For increasing ^{3}He coverage, the transition from a 2DFG to a 3DFG was found to be smooth and did not show any structure. In the last decade, starting with a series of experiments by Bhattacharyya, Gasparini, and Di Pirro,[3] finite-size effects have been investigated by considering thin ^{4}He films. The results on the heat capacity of the fermions point to the existence of several types of states accessible to the ^{3}He atoms. More recently, Higley et al.[4] have observed clear steps in the magnetization of ^{3}He impurities on thin films of ^{4}He. The first step was interpreted as due to an excited state 1.8 K above the ground state.

The relation between the structure of the states on the surface of the bulk and on thin films has been investigated by Sherrill and Edwards.[5] In their model, there is only one state localized in the surface of the bulk. Their results concerning the films can be summarized by considering the two relevant effects coming into play, namely i) the potential of the substrate and ii) the finiteness of the film. The surface state is rather insensitive to the thickness d of the film, and consequently its energy decreases with d due to the attractive tail of the substrate potential. In contrast, the states representing a ^{3}He atom dissolved in the bulk ^{4}He (with energy −2.8 K) are subject to a quantum finite-size effect. They give rise to discrete states, with energy *larger* than −2.8 K. In the limit of very thin films, though, the attractive substrate potential becomes large enough to overcome this finite-size effect, and all energies decrease with d. Anderson and Miller[6] have obtained recently similar results. Consequently, these studies predict that, in films, the energy interval between the ground state and the first excited state is *larger* than in the bulk surface, i.e., larger than 2.2 K. From the work of Sherrill and Edwards, one obtains an energy interval of ~4.5 K for the film considered in Ref. 4. From Ref. 6, one obtains a value of ~3 K. These values are in clear contradiction with the findings of Higley et al. mentioned above, i.e., 1.8 K.

Recently, Krotscheck and coworkers have undertaken the task of investigating static and dynamical properties of inhomogeneous helium at zero temperature using the hyper-netted chain (HNC) approximation. Concerning helium films,[7,19] they provide the more microscopic results presently available. They exhibit an extremely interesting and important feature, the layering of the ^{4}He film produced by the strong substrate potential. However, these calculations provide only a semiquantitative description because, as is well known, the HNC approximation is poorly converging for liquid helium.[7] The equilibrium density and energy per atom of pure liquid ^{4}He at zero temperature and pressure are underestimated by 30% and the surface tension by a factor of two[7a]; also,[7b] the ^{3}He surface state seems to converge, for thick films, to a value at least 1.5 K above the quoted value of −5 K. Hence, the quantitative predictive power of the theory is somewhat limited, and we

shall see below that, concerning the ^{3}He impurity states, this may also have some *qualitative* consequence.

In the present work, we propose an interpretation of the results of Ref. 4 based on the possibility that the bulk ^{4}He surface accommodates *more than one* ^{3}He surface state. This idea is substantiated by a recent study by Dalfovo and Stringari,[8] further developed in Ref. 9. As shown in Ref. 8, the number of surface states accessible to a ^{3}He impurity is related to the surface width of the ^{4}He liquid. The larger its value, the less confining it is for a ^{3}He atom, hence more binding. The value of 7 Å found in Ref. 11 and also by Pandharipande *et al.* in large clusters[10] is significantly larger than in the work of Sherrill and Edwards ($\sim$4 Å), who used the ^{4}He surface profile deduced from a study of the scattering of ^{4}He atoms by the free surface.[12] However, it was clearly shown in Ref. 12 that the scattering of ^{4}He atoms was only loosely related to the full width of the surface *density*, being mainly determined by the asymptotic behavior of the *average field*. Hence, we feel that it is worth considering the possible consequences of a larger ^{4}He surface thickness.

The physical picture discussed here is the following: if there are several types of surface states accessible to the ^{3}He atoms, then their energy will not be very sensitive to the finiteness of the film; they will be sensitive (almost equally) to the attractive tail of the substrate potential, so that the energy difference between the first and second state will remain roughly constant. As the energy difference between the ground state and the first excited state found in Refs. 8 and 9 is 1.8 K, one may have here an explanation for the results of Ref. 4.

The method used in Refs. 8 and 9, however, is not adequate to calculate thin films on a substrate; inhomogeneities are dealt with through gradient expansions that are not legitimate in the present case for two important draw-backs, namely, (i) the high external pressure due to the substrate creates a spatial ordering of the liquid (the layered structure calculated by Krotscheck and coworkers), which occurs with a characteristic length related to the hard core of the interatomic potential, and gradient expansions miss this microscopic characteristic length, and (ii) the effective interaction derived from the simple functional of Refs. 8 and 9 has, in momentum space, a k^2 dependence unrealistically large at large k's: such a model is not accurate for the strong inhomogeneities of the fluid near the substrate.

For these reasons we have developed a new method which, while keeping the simplicity of a density functional approach, is able to describe perturbations of the liquid on a microscopic scale (Sec. 2). We use it in Sec. 3 to calculate the structure of mixture films. The comparison with experiment is given in Sec. 4. Our conclusion are summarized in Sec. 5.

2. A DENSITY FUNCTIONAL APPROACH WITH A FINITE RANGE INTERACTION

We have used an extended version of the method proposed in Ref. 13 for the case of pure ^{4}He, which we now briefly recall. The physical idea underlying the construction of the density functional is to define, in the interatomic potential, a long-range part, which is treated in a mean-field approximation, and to represent the effect of the short-range correlations by a density dependence. As a guide, one imposes that the experimental pressure-density relation of the uniform medium at zero temperature be correctly reproduced.

The energy of a given volume V of the ^{4}He fluid in the external potential $V_{\text{ext}}(\mathbf{r})$ is written as

$$E = \int d^3r \frac{\hbar^2}{2m_4} |\nabla \phi_4(\mathbf{r})|^2 + \tfrac{1}{2} \int d^3r\, d^3r'\, \rho_4(\mathbf{r})\rho_4(\mathbf{r}')V_4^l(|\mathbf{r}-\mathbf{r}'|)$$

$$+ \tfrac{1}{2}c_4 \int d^3r\, \rho_4(\mathbf{r})[\bar{\rho}_4(\mathbf{r})]^{1+\gamma_4} + \int d^3r\, V_{\text{ext}}(\mathbf{r})\rho_4(\mathbf{r}) \qquad (1)$$

where $\phi_4(\mathbf{r}) = \rho_4(\mathbf{r})^{1/2}$ and m_4 is the mass of a ^{4}He atom.

The first term in the rhs of Eq. (1) represents the usual inhomogeneity correction to the quantum kinetic-energy density. The second term represents the contribution to the energy of the long-range part of the interatomic interaction. It is natural to take for V_4^l the standard Lennard-Jones potential describing the ^{4}He–^{4}He interaction ($\varepsilon = 10.22$ K, $a = 2.556$ Å), screened in a simple way at distances shorter than a characteristic distance h_4 (let $x = |r - r'|/a$)

$$V_4^l(|\mathbf{r}-\mathbf{r}'|) = \begin{cases} 4\varepsilon(x^{-12} - x^{-6}) & \text{for } |\mathbf{r}-\mathbf{r}'| \geq h_4 \\ V_4^l(h_4)(ax/h_4)^4 & \text{for } |\mathbf{r}-\mathbf{r}'| < h_4 \end{cases} \qquad (2)$$

The shape of the screened core potential (2b) has been taken as a power law. The choice of the fourth power is not critical (see discussion of Ref. 13).

In the third term of Eq. (1), $\bar{\rho}_4(\mathbf{r})$ is the local density averaged over a sphere centered at $\mathbf{r}$ with a radius h_4: $\bar{\rho}_4(\mathbf{r}) = \rho_4 * \Pi_{h_4}$ (the star denotes the convolution of two functions) with $\Pi_{h_4}(\mathbf{r}) = 3\theta(r - h_4)/(4\pi h_4^3)$, where θ is the Heaviside function. The form of this term is inspired by the "smoothed density approximation" introduced in studies of classical fluids by Tarazona.[14] It accounts for the internal kinetic energy as well as for increasing contribution of the hard core when the density is increasing. When $\bar{\rho}_4(\mathbf{r})$ is expressed in term of $\rho_4(\mathbf{r})$, it appears clearly to describe many-body correlations with a range of order h_4.

For uniform density, in the absence of an external field, the energy of the liquid is equal to

$$V\left(\frac{b_4}{2}\,\rho_4^2+\frac{c_4}{2}\,\rho_4^{2+\gamma_4}\right)\tag{3}$$

We take the values of c_4 and γ_4 from Ref. 8, and choose h_4 so that the integral of the long-range part of the potential V_4^l, i.e., b_4 in Eq. (3), gives the same value as in Ref. 8. This ensures a correct pressure-density relation over a wide range of densities.

The static density–density response function obtained with this method is in good agreement with the measurements of Cowley and Woods.[15] When applied to the description of the free surface of liquid ⁴He, it gives the experimental surface tension and a surface width of 5.8 Å, i.e., slightly smaller than in Refs. 10 and 11. The scattering of ⁴He atoms by the free surface comes out also in agreement with experiment,[12,16,17] despite the fact that the surface width of the density is significantly larger than that assumed by Edwards and coworkers.

The density distribution of a film is given by minimizing the energy, submitted to the constraint of a given areal density, for the specific geometry we are interested in: the interface is taken as flat, parallel to the x-y plane, with the substrate located at $z=0$. The Euler equation for ϕ_4 then reads as

$$-\frac{\hbar^2}{2m_4}\,\frac{d^2\phi_4(z)}{dz^2}+[U_4(z)+V_{\text{ext}}(z)]\phi_4(z)=\mu_4\phi_4(z)$$

$$U_4(z)=\rho_4*V_4^l+\frac{1+\gamma_4}{2}\,c_4(\,\rho_4\,\bar\rho_4^{\gamma_4})*\Pi_{h_4}+\frac{c_4}{2}\,\bar\rho_4^{1+\gamma_4}\tag{4}$$

where μ_4 is the chemical potential of a ⁴He atom.

The interaction between the helium atoms and the substrate is represented by a Lennard-Jones potential which, once integrated over a half-space, gives an external potential

$$V_{\text{ext}}(z)=e\left[\frac{1}{15}\left(\frac{\sigma}{z}\right)^9-\frac{1}{2}\left(\frac{\sigma}{z}\right)^3\right]\tag{5}$$

In Eq. (5), σ denotes the position of the hard core of the substrate atom-helium atom Lennard-Jones potential; notice that in Ref. 7b, the external potential is written equivalently in terms of the position s of the minimum at the potential, related to σ by $\sigma=s/2^{1/6}$.

The extension of the present approach to helium mixtures is straightforward. We start with the parametrization of the bulk properties of ³He–⁴He mixtures proposed in Ref. 18 by Dalfovo and Stringari and define nonlocal

generalizations analogous to the case of pure ^{4}He. The long-range part of the ^{3}He–^{3}He and ^{3}He–^{4}He potential is naturally taken to be the same Lennard-Jones potential as for pure ^{4}He, screened, however, at distances h_3 and h_{34}, respectively, such that the integral of the potential gives the coefficients b_3 and b_{34} of Ref. 18. In the following we refer to these long range potentials as V_3^l and V_{34}^l. We then use the smoothed density approximation to generalize the density dependent terms representing the short-range correlations. In doing so, one preserves the various properties correctly parametrized in Ref. 18. In particular the effective mass of a ^{3}He atom in liquid ^{4}He has the same form as in Ref. 18, with the weighted densities replacing the local densities. In the limit of infinite ^{3}He dilution, it reads

$$\frac{\hbar^2}{2m_3^*(\mathbf{r})} = \frac{\hbar^2}{2m_3}\left(1 - \frac{\bar{\rho}_4(\mathbf{r})}{\rho_{4c}}\right)^2 \tag{6}$$

The total functional describing the ^{3}He–^{4}He mixture in the limit of zero ^{3}He concentration is explicitly

$$E = \int d^3r \frac{\hbar^2}{2m_4}|\nabla\phi_4|^2 + \frac{1}{2}\int d^3r\, d^3r'\, \rho_4(\mathbf{r})V_4^l(|\mathbf{r}-\mathbf{r}'|)\rho_4(\mathbf{r}')$$

$$+ \frac{c_4}{2}\int d^3r\, \rho_4\bar{\rho}_4(\bar{\rho}_3 + \bar{\rho}_4)^{\gamma_4} + \int d^3r \frac{\hbar^2}{2m_3^*}|\nabla\phi_3|^2$$

$$+ \int d^3r\, d^3r'\, \rho_3(\mathbf{r})V_{34}^l(|\mathbf{r}-\mathbf{r}'|)\rho_4(\mathbf{r}') + \frac{c_{34}}{2}\int d^3r(\bar{\rho}_3\rho_4 + \rho_3\bar{\rho}_4)\bar{\rho}_4^{\gamma_{34}} \tag{7}$$

$$+ \int d^3r(\rho_3 + \rho_4)V_{\text{ext}}$$

where $\bar{\rho}_3(\mathbf{r}) = \rho_3 * \Pi_{h_3}$. The function Π_{h_3} is defined similarly to Π_{h_4}.

The values obtained for the lengths h_3, h_4, and h_{34} are

$$h_3 = 2.3563 \text{ Å}$$

$$h_4 = 2.3767 \text{ Å}$$

$$h_{34} = 2.3653 \text{ Å}$$

The values of the other parameters defining the functional of Eq. (7) are gathered in Table I. They yield correct values of the effective mass, of

TABLE I

Values of the Parameters Defining the Energy Density Functional, Eq. (7)*

γ_4	$c_4\rho_0^{1+\gamma_4}$ [K]	γ_{34}	$c_{34}\rho_0^{1+\gamma_{34}}$ [K]	ρ_{4c} [Å^{-3}]
2.8	5.1074	2.5	7.023	0.062

*The γ's have no dimension. $\rho_0 = 0.021836$ Å^{-3}.

the chemical potential, and of the excess volume parameter of the mixed system over a wide range of pressure. Notice that these properties concern only homogeneous mixtures and that no experimental information on inhomogeneous systems is introduced in the functional.

The various states accessible to ^{3}He impurities on a ^{4}He film are obtained by varying the energy of the system, Eq. (7), with respect to the wavefunction ϕ_3. A Schrödinger-type of equation, with a mass depending on position, results

$$-\frac{d}{dz}\left(\frac{\hbar^2}{2m_3^*}\cdot\frac{d\phi_3^i}{dz}\right)+(U_3(z)+V_{\text{ext}}(z))\phi_3^i(z)=\varepsilon_i\,\phi_3^i(z)$$

(8)

$$U_3(z)=\rho_4*V_{34}^I+\frac{\gamma_4}{2}\,c_4(\,\rho_4\,\bar{\rho}_4^{\gamma_4})*\Pi_{h_3}+\frac{c_{34}}{2}\,(\,\bar{\rho}_4^{1+\gamma_{34}}+(\,\rho_4\,\bar{\rho}_4^{\gamma_{34}})*\Pi_{h_3})$$

where the Lagrange multiplier ε_i, introduced in order to satisfy the condition of normalization of the wave function, appears as the energy of the state. From the solution of Eq. (8), one can also calculate the effective mass M_i of a ^{3}He atom in each state, defined as

$$\frac{\hbar^2}{2M_i}=\int_{-\infty}^{+\infty}dz\,\frac{\hbar^2}{2m_3^*(z)}\,|\phi_3^i(z)|^2$$

(9)

Different numerical methods are used to solve Eqs. (4) and (8). Equation (4) is a ground-state problem for which we use the "imaginary time step method" presented in Ref. 13. One first solves the equation for a mean field $U_4(z)$ constructed from a trial density, and self-consistency is achieved by recalculating the field with the new solution and repeating the procedure until convergence is achieved. Three stable significant digits on the chemical potential are obtained with typically 200 iterations of the first kind and 150 iterations for self-consistency. This method would be cumbersome to apply for the determination of the numerous impurity states. Moreover, the careful procedure we use to solve Eq. (4) is not necessary here, since Eq. (8) has no self-consistent field and is the usual linear Schrödinger equation. One therefore proceeds as follows: starting with an initial guess for the energy, one integrates Eq. (8) (using a fourth-order Runge–Kutta method) from the origin to a given matching distance z_c and then from an asymptotically large z backwards to z_c. Asking for equal values of the logarithmic derivatives of the solutions at $z=z_c$ provides an algorithm able to determine the energy of the eigenstate. One stops the iterations when three stable digits are obtained for the energies and the effective masses. Greater accuracy is reached when the matching point is chosen where the gradient of the density is large, for example, at the surface of the film. By scanning the energy interval between

the bottom of the field and zero, one determines all the states. By counting the number of zeros of the wavefunctions, one checks that no state has been missed.

3. RESULTS AND DISCUSSION

The structure of the films depends of course on the substrate potential, which is characterized by two parameters in Eq. (5). In the case of Nuclepore, which is the substrate we are interested in, the long range attractive tail in $1/z^2$ has an intensity of about 1860 K. The short range repulsion determining the depth of the potential well is less known, due in particular to the corrugation of the surface. Indeed, the first helium atoms, rather than forming a film, will first fill the dips existing at the surface, and when a translationally invariant film starts forming (which is the structure we calculate), the effective substrate is a complicated medium made of Nuclepore and helium atoms in the dips. How many atoms are trapped is difficult to evaluate, but their effect is probably to weaken the attractive potential well, because the helium–helium interaction is so weak. Inasmuch as we do not describe the trapped atoms, one may expect a shift in coverage between calculated and observed properties of the films. Also, the fact that the substrate potential is not really invariant parallel to the surface is equivalent to considering a distribution of potentials, the effect of which is to give some width to the impurity states. This is how the authors of Ref. 4 have analyzed their data, and the width of the first excited state came out to be of the order of 0.1 K. In the following, we have chosen the values

$$\sigma = 3.21 \text{ Å}$$

$$e = 113 \text{ K}$$

which gives a potential 20% less attractive than the potential of Ref. 7b, and about twice less attractive than graphite. A systematic study for various substrates will be presented in a forthcoming paper. The present results should be considered as representative of a moderately attractive potential.

Figure 1 shows the ^{4}He density profile for ^{4}He films with coverage in the range $N_4 = 0.15$ Å^{-2} to 0.70 Å^{-2}, together with the corresponding average field $U_3(z) + V_{ext}(z)$ experienced by a ^{3}He atom. Three different types of films can be identified: for $N_4 < 0.20$ Å^{-2}, the structure of the film is determined essentially by the substrate potential, and we shall refer to this situation as *wall-dominated*. For $N_4 \geq 0.50$ Å^{-2}, one recovers a liquid similar to the bulk free surface where the average field exhibits the characteristic well of the *asymptotic* regime, as in Refs. 8 and 9. For intermediate coverage,
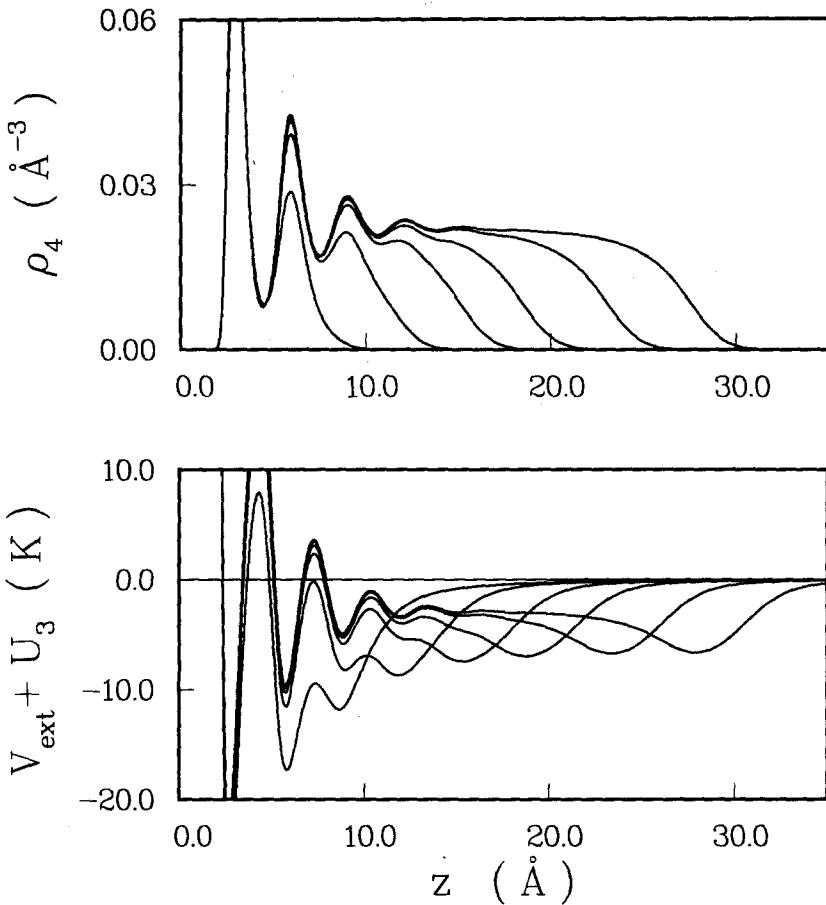
Fig. 1. Upper part: ⁴He density profile for films with coverage of 0.150, 0.240, 0.325, 0.400, 0.500, and 0.600 $Å^{-2}$. Lower part: corresponding average field experienced by a ³He atom.

one has a *transition* structure, where the surface of the liquid is still perturbed by the substrate and where the surface potential well is developing. In all cases, close to the substrate, one obtains a layered structure similar to that of Refs. 7 and 19, with five visible oscillations of the density. Notice that the completion of a given layer occurs for a coverage for which the next layer already starts being formed.

For large films, the compression obtained in the first two layers is 4.2 and two times the saturation density; the number of atoms in the first layer (from the origin to the first minimum) is 0.98 $Å^{-2}$ and in the second layer (from the first minimum to the second one), 0.76 $Å^{-2}$. Due to the corrugation of the surface, these numbers are difficult to compare with experiment,

but in the case of a graphite substrate ($e = 210$ K and $\sigma = 2.74$ Å in Eq. (5)), for which the corrugation is certainly small, one obtains respectively 0.114 Å^{-2} and 0.090 Å^{-2}; these values agree nicely with those of Ref. 20. This agreement does not mean that the description of the first layer is realistic. The compression near the wall is such that this layer is certainly solid (i.e., the density is strongly modulated in the x-y plane), and this is neglected in our calculation where we impose translational invariance parallel to the surface. However, the fact that the number of atoms in this layer is correct indicates that the approximation may not affect too much the potential felt in the second layer and beyond.

In Fig. 2 we have plotted the variation of the binding energies ε_i of a ^{3}He atom as a function of N_4. We confirm the results obtained in Refs. 8 and 9 that the bulk surface can support *two* surface states, with energies
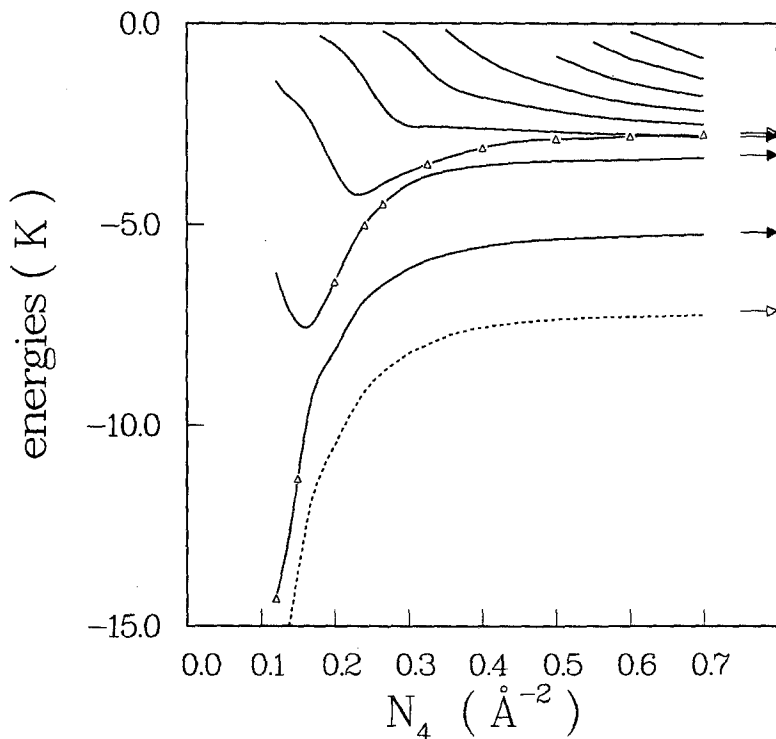

Fig. 2. Solid lines: energies of the various ^{3}He states, for N_4 in the range 0.12 to 0.70 Å^{-2}. Triangles indicate the substrate state (eigenstate most localized near the substrate). Note that the position of this state in the sequence of states is a function of film thickness. The asymptotic values indicated by a black arrow are -5.20, -3.16, and -2.80 K. The open arrow corresponds to the substrate state, with asymptotic value -2.72 K. Dashed line: ^{4}He chemical potential, with asymptotic value -7.15 K (open arrow).

-5.20 and -3.16 K, compared to the values -5.4 and -3.6 K of Refs. 8 and 9. The differences are related to the smaller ⁴He surface width obtained with a finite-range force, which confines slightly more the ³He impurity. Apart from the wall-dominated films, one finds three states more influenced by the attractive potential than by the finiteness of the film so that, down to $N_4 \simeq 0.20$ Å^{-2}, their energy decreases for smaller coverage. As indicated in the introduction, this behavior, qualitatively similar to that obtained by Sherrill and Edwards for their surface state, was expected. The important consequence is that down to a coverage of $N_4 \simeq 0.25$ Å^{-2}, the energy intervals depend weakly on N_4, $\Delta\varepsilon_1 = \varepsilon_1 - \varepsilon_0 = 1.8$ to 2 K and $\Delta\varepsilon_2 = \varepsilon_2 - \varepsilon_1 \simeq 0.4$ to 0.6 K. For thinner films, $\Delta\varepsilon_1$ exhibits a minimum of 1.6 K for $N_4 \simeq 0.22$ Å^{-2} and then increases strongly, because the first excited state becomes sensitive to the finiteness of the film. A similar behaviour is seen for $\Delta\varepsilon_2$, with a minimum of 0.2 K for $N_4 \simeq 0.275$ Å^{-2}. The ground state energy ε_0 and the chemical potential μ_4 show structures for $N_4 \simeq 0.15$, 0.22, and, though less pronounced, 0.30 Å^{-2}. These coverages correspond to values slightly below the completion of the second, third, and fourth layer, i.e., before the formation of the next layer. The structures in the chemical potential are qualitatively similar to those obtained by Epstein et al.[19] Their effect on the velocity of third sound will be studied elsewhere. We shall see below that the completion of the second and third layer can also be seen in the ground-state effective mass.

It is interesting to examine the wave functions associated with each state. Figure 3 presents three cases: an asymptotic large film with $N_4 = 0.60$ Å^{-2}, a wall-dominated film of 0.15 Å^{-2}, and an intermediate case of 0.24 Å^{-2}. The four first states of the thick film, shown in the lower part of Fig. 3, illustrates the three type of states which can be identified, namely, (i) surface states, for which the wavefunction is localized in the surface region (in the present case, the two lower states), (ii) film states, which extend throughout the film (the fourth, fifth ... states), and (iii) a type of state which appears in all film, localized near the substrate in the second layer of the film (in Fig. 3c, it is the third state), to which we shall refer as the *substrate state*. The distinction between film states and surface states becomes of course less relevant in wall-dominated films, but the substrate state can be clearly identified in all cases. The position of the substrate state, in the sequence of available states, changes as indicated in Fig. 2 by the open triangle. This is also illustrated by the comparison between the two thinnest films in Fig. 3; in wall-dominated films, the ground state is the substrate state; as the thickness increases, the substrate state becomes the first excited state, while the ground-state wavefunction moves out to the surface and becomes a surface state. This feature, as we shall see, is the key to the understanding of a number of experimental data on thin mixture films.
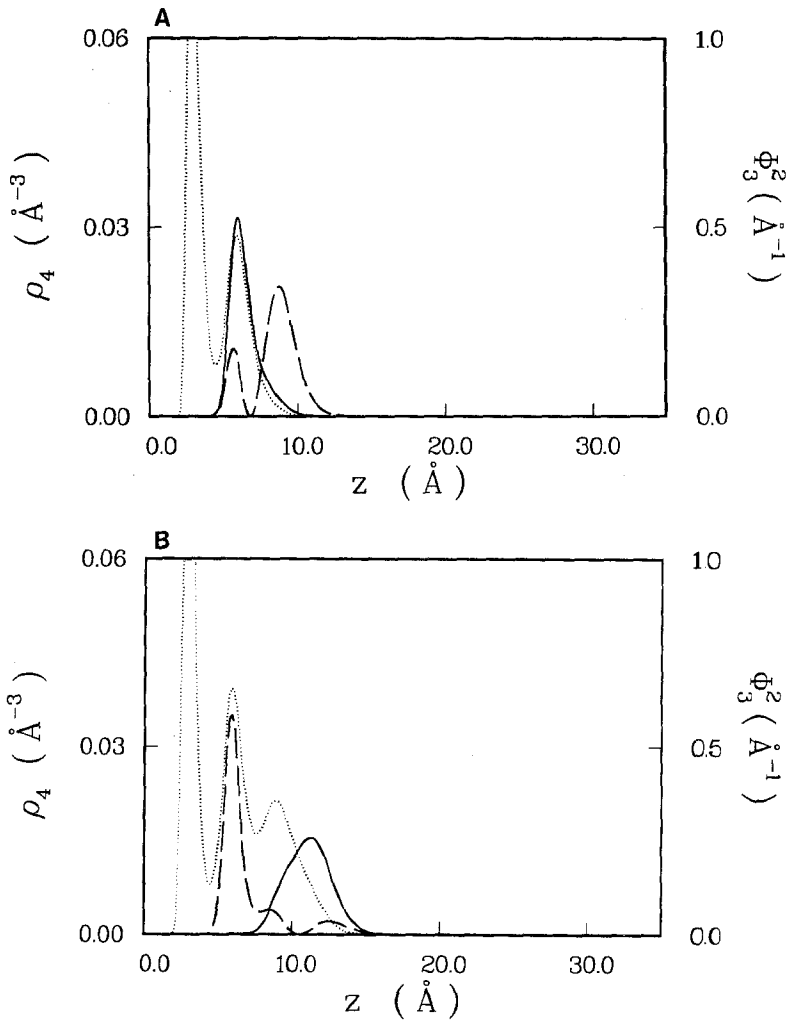
Fig. 3. Normalized ³He wavefunctions (squared), for ⁴He coverage of 0.15, 0.24, and 0.6 Å⁻². Only the two first states are shown in (A) and (B) (solid line: ground state; long-dashed line: first excited state). In the asymptotic film of (C) are shown the first four states (dashed line: second excited state; short-dashed line: third excited state). In all cases, the ⁴He density profile is represented by the dotted line.

The localization of the wavefunctions explains the variation of the effective mass associated with each state as a function of film thickness, as shown in Fig. 4 for the first four states. The asymptotic values of the effective mass of the two surface states are found to be $1.35m_3$ and $1.74m_3$ respectively; for a film state, it is equal to the known value $2.38m_3$ of a ³He atom
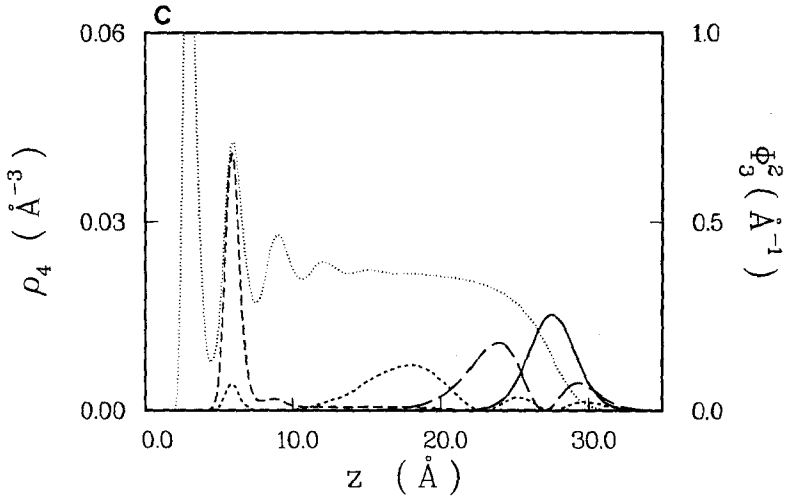
Fig. 3. Continued.

dissolved in the bulk ^{4}He liquid; for the substrate state, one finds a value of $2.87m_3$. As indicated above, when the thickness of the film increases, the position of the substrate state moves up in the sequence of available states; this produces a maximum in the effective mass of the first four states, reached when that particular state becomes the substrate state. (M_0 has the particularity of having *two* maxima, the first one for a coverage of 0.15 Å^{-2} and a smaller one for 0.2 Å^{-2}. The first one corresponds to the completion of the second layer of the film, where is localized the ground-state wave function. Then, for increasing ^{4}He coverage, a third layer develops, while the ground state becomes a surface state; hence the completion of this third layer reflects in M_0.) The maximum is larger M_1 than in M_0, larger in M_2 than in M_1, etc...., because the substrate state wavefunction has a tail, as can be seen in Fig. 3, which explores the liquid beyond the second layer. Hence, the corresponding effective mass saturates only when the profile of the film does not change any more over the first few oscillations, which occurs only for N_4 larger than 0.50 Å^{-2}. Let us notice that our results for M_0 are very similar to those recently obtained by Epstein *et al.*[19] This agreement validates Eq. (9), indicating that the effective mass in *two dimensions* can be calculated by averaging the *bulk* effective mass with the appropriate two-dimensional probability density.

The existence of the substrate state is a new result of the present work, and we have seen that it is an important feature of the structure of states. It is linked to the increase of the ^{3}He effective mass with increasing ^{4}He density; the resulting decrease of the kinetic energy compensates the effect of the localization of the ^{3}He atom in that state. In particular use of the bare
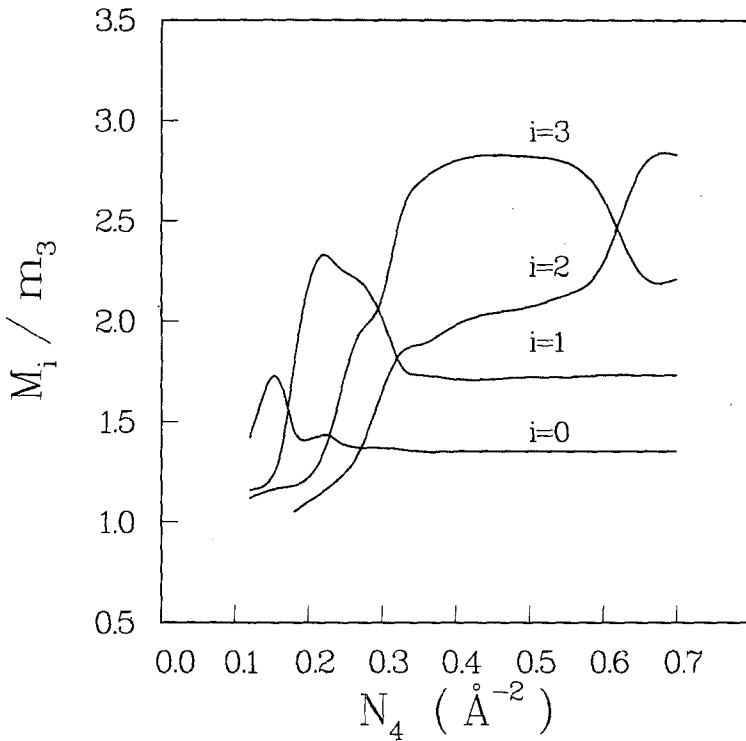
Fig. 4. Variation of the effective mass of the first four states with ^{4}He coverage in the range 0.12 to 0.70 Å^{-2}. The asymptotic values are 1.35, 1.74, and 2.38 for the two surface states and the bulk state, respectively. The asymptotic value for the substrate state is 2.87.

mass m_3 in Eq. (8) makes this state disappear. Asymptotically, the energy of the substrate-state is found to be slightly above -2.8 K, the energy of a ^{3}He atom dissolved in the bulk ^{4}He. The precise value is of course directly related to the value of the strength of the Nuclepore-helium interaction, which is not known with a great accuracy. Also, keeping the attractive part constant in Eq. (5) and changing the repulsive part will affect the energy of the substrate state. In order to test its sensitivity, we have arbitrarily increased the value of e in Eq. (5) from 40 K to 50 K; the asymptotic energy of the substrate state is decreased by 0.5 K.

Let us now turn to a brief comparison of our results with the work of Krotscheck and coworkers. Qualitatively, both approaches lead to similar features: the layering produced by the substrate potential, the decrease of the first two ^{3}He eigenstates with decreasing thickness, and the structure of the ground state effective mass. There are minor quantitative differences in

the results that are simple consequences of the fact that the HNC approxima-
tion does not reproduce accurately the properties of liquid helium; for exam-
ple, as the HNC equilibriuim density is 0.017 Å^{-3}, a film with a given
coverage is thicker than it should (for $N_4 \simeq 0.30 \text{ Å}^{-2}$, the HNC calculation
predicts that the fifth layer is forming; in our approach, it is only the fourth
one). The lack of binding energy in the HNC calculation (-5.4 K instead of
-7.15 K for pure liquid ⁴He) reflects also in the chemical potential μ_4 of the
films. For the substrate potential of Ref. 7b and for a coverage of 0.30 Å^{-2},
the present method gives $\mu_4 = -8.55$ K, whereas the HNC result is about
-6 K. That the equation of state is responsible for the difference is proven
by the fact that, by fitting a density functional to the HNC bulk properties
of helium (as it is done to the experimental ones), one recovers a value $\mu_4 =$
-6.2 K and a density profile very similar to the HNC profile. More impor-
tant is that the *quantitative* defficiency of the HNC approximation, which
was recognized in Ref. 7, has, in the present context, two *qualitative* conse-
quences. First, it seems, from the results of Ref. 7b, that thick films will
support only *one* ³He surface state; indeed, in the thickest film, for which
the asymptotic regime is clearly not yet reached, the energy of the first exicted
state (-2.47 K) is larger than that of a ³He atom dissolved into the bulk
(-2.60 K in the HNC approximation). Second, although the HNC wave-
functions of certain excited states extend into the second layer of the film, a
substrate state as found in the present work is not predicted in Ref. 7b.
These differences with our results point to differences in the impurity poten-
tial, which is more attractive in our case: the pocket of potential correspond-
ing to the position of the second layer of the liquid is of the order of 5 K
deeper; in the surface region, our potential is deeper by 2 K (see Fig. 2 of
Ref. 7b). Of course our approach is less fundamental than that of Ref. 7b;
but its phenomenological character has some advantage: as a number of
physical properties of the system are built in (bulk properties of dilute mix-
tures) or are correctly described by the model (e.g., its surface tension), one
may have some confidence in the impurity potential. As an indication, the
asymptotic value of the binding energy of a ³He atom agrees with the exper-
imental value.

4. COMPARISON WITH EXPERIMENT

The results discussed in the preceeding section are obtained in the limit
of zero ³He coverage, so that the comparison with experiments performed
for finite coverages necessitates an extrapolation which is not easily done.

Conversely, one may try to anticipate the dependence of our results on
³He coverage. For thick films, one can rely on the results of Ref. 9 obtained
for ³He impurities on the bulk surface. They indicate that (i) the energy of

the ground state increases by 0.5 K for a ^{3}He coverage of one layer while the energy of the first excited state remains almost constant and (ii) the effective mass of the ground state increases by 25% and that of the first excited state by 6% for one layer of ^{3}He atoms. In thin films, the situation is more complex; as the wavefunction of each state are distributed differently, interaction effects will act differently on each state. For example, filling the continuum built on the substrate state should expel ^{4}He atoms from the second layer, thus increasing the film thickness and consequently the surface state energies. In contrast, filling the continuum built on a surface state should not affect the energy of the substrate state. As a result, the energy difference between the ground state and the first excited state may be quite dependent on coverage for $N_4 < 0.35$ Å^{-2}. There are nevertheless a number of qualitative and semiquantitative features that are not expected to be changed by interaction effects and that explain several independent sets of experiments.

The first attempts to determine the energies and effective masses of the first two states of a mixture film were made by specific-heat measurements and are reported in Ref. 3. In the classification introduced in Sec. 4, these films correspond to transition and asymptotic films, i.e., $N_4 > 0.35$ Å^{-2}. From Figs. 14 and 17 of Ref. 3, it appears that the energy gap $\Delta \varepsilon_1$ between these two states tends to a value 1.7 to 1.8 K. Although the possibility of a bulk surface accommodating more than one surface state was not considered in Ref. 3, it seems to us that the data point to, or at least do not contradict, such a structure. To the contrary, the values of $\Delta \varepsilon_1$ for the thinnest films considered in Ref. 3 extrapolate for zero ^{3}He coverage to numbers larger than ours by a factor of two. These results are to be contrasted with the recent determination $\Delta \varepsilon_1 \simeq 1.6$ to 1.8 K by Higley et al.,[4,21] in films of ^{4}He coverage in the range 0.240 to 0.325 Å^{-2}. The agreement with our calculations is satisfactory, and our Fig. 2 may also explain why only two steps were identified in the magnetization, the fourth level in these films being $\simeq 3$ K above the third one. The observation of the second step for a ^{3}He coverage of 1.5 layers indicates also that the second energy interval $\Delta \varepsilon_2$ is significantly smaller than $\Delta \varepsilon_1$, in agreement with our findings.

Concerning the effective mass, our curve for M_0 shows the same structure as in Ref. 22, where are gathered results from specific heat and surface tension measurements for thick films, and from oscillator mass loading for thin films. The maximum is seen for the same coverage of 0.15 Å^{-2} that, as explained in the previous section, corresponds to the completion of the second layer and a ground state still located in this layer. One expects interaction effects to shift our values upward,[9,19] bringing the calculated values in agreement with experiment. A similar increase of M_0 with decreasing thickness is reported by Higley et al., however, with a stronger thickness dependence. Observation of the structure in M_1 would be a strong confirmation of

the present picture, i.e., of the promotion, with increasing coverage, of the substrate state as an excited state.

The structure of states shown in Fig. 2 and the localization of the corresponding wavefunctions provide also an alternative explanation to the layered-mixed transition reported in ref. 23 and analyzed in terms of inter-facial fluctuations. By measuring third-sound velocities in thin mixture films, the authors of Ref. 23 were able to attribute its variation with ⁴He coverage to a change in the structure of the films: thin films were found homogeneous while in thicker films a phase separation was identified. The transition from homogeneous to layered mixture films can be simply understood in the framework of the present results: for a ³He coverage of the order one atomic layer, one expects the first two types of states to be occupied. For a ⁴He coverage of two atomic layers, which is the thinnest film considered in Ref. 23, Fig. 3 indicates that the ground state is localized in the surface and the first excited state is the substrate state. Hence, the mixture film appears as homogeneous. For four atomic layers, the first two states are now localized in the surface, and this appears as a phase separation, the ³He atoms being now on top of the liquid.

Another set of experiments for which the present results may be relevant is discussed in Ref. 24, where a decrease of ~10% of the third-sound velocity in relatively thick mixture films is reported to take place between $T=0.15$ mK and $T=0.20$ mK, for ³He coverages around four layers. Hallock speculated that "this step may be caused by a dramatic purge of the ³He out of the surface blanket into the ⁴He film with a consequent lowering of the third-sound velocity."[24] The present results provide such a mechanism. In thick films, the substrate state being third or fourth state, it is possibly not occupied at low temperature, even with four layers of ³He; the thermal promotion of the ³He atoms into the substrate state is then able to produce the observed effect. The temperature for which the *purge* occurs is determined by the energy difference between the ³He Fermi energy and the energy of the substrate state. This requires the calculation of the dependence of the impurity states on ³He coverage.

5. CONCLUSION

In the present work, we have developed a density functional theory that is able to describe the formation of layers of compressed ⁴He liquid close to a substrate and the evolution with film thickness of the states accessible to ³He impurities. The parameters of the functional are fitted to *bulk* properties of dilute mixtures, without incorporating any experimental

information on inhomogeneous systems. The long-range part of the inter-
atomic potential is treated in a mean field approximation, and short-
range correlations are dealt with through a density dependence. The
essential results emerging from this study are: (i) the existence of two
surface states localized in the surface of thick films, with asymptotic
energies and effective masses $(-5.20 \text{ K}, 1.35)$ and $(-3.16 \text{ K}, 1.74)$; (ii) the
energy difference between the ground state and the first excited state
remains, down to a coverage of $N_4 \simeq 0.20 \text{ Å}^{-2}$, in the range 1.6 to
2.2 K, in agreement with the recent determination from magnetization
measurements[4,21]; (iii) the existence of a state close to the substrate (in
the second layer of the film); its position in the sequence of available
states varies with thickness, from the ground state in thin films to a value
close to the binding energy of a ^{3}He atom dissolved in the bulk. (iv) the
effective mass associated with the ground state has a maximum for a ^{4}He
coverage of 0.15 Å^{-2}, in agreement with experiment[3,22] and with recent
microscopic calculations[19]; similar maxima are predicted to exist for the
effective mass of the first few states, corresponding to coverages for which
each of these states becomes the substrate state.

The two surface states found in the present study confirm the findings
of previous studies using simpler phenomenological methods[8,9] for the bulk
surface. This structure is expected to produce steps in the surface specific
heat.[9] Direct observation of the states should be possible by studying the
emission of ^{3}He atoms by phonons generated in the bulk liquid and hitting
the surface.[25]

Concerning the substrate state, we have indicated several experimental
hints pointing to its existence. Its identification could be more directly looked
for by considering systems where the surface states are absent: this can be
obtained by simply filling up the pores of the substrate so that there is no
longer a free ^{4}He surface. ^{3}He impurities added to the liquid would then
occupy either the substrate state or the state extending throughout the liquid,
depending on which has the lower energy. Also, changing the pressure in
the liquid should affect more the liquid state than the substrate state; one
may thus have a way of controlling the relative position of the two energies,
and consequently, the dimensionality of the system. In any case, the poss-
ibility of forming a new two-dimensional Fermi liquid near the wall, on the
basis of the present results, should be explored.

REFERENCES

1. A. F. Andreev, *Zh. Eskp. Teor. Fiz.* **50**, 1415 (1966) [*Sov. Phys. JETP* **23**, 939 (1966)].
2. D. O. Edwards and W. F. Saam in *Progress in Low Temperature Physics*, D. F. Brewer, ed. (North-Holland, Amsterdam, 1978), vol. VIIA, p. 283.
3. B. K. Bhattacharyya, M. J. Di Pirro, and F. Gasparini, *Phys. Rev. B* **30**, 5092 (1984), and references therein.
4. R. H. Higley, D. T. Sprague, and R. B. Hallock, *Phys. Rev. Lett.* **63**, 2570 (1989), and references therein.
5. D. S. Sherrill and D. O. Edwards, *Phys. Rev. B* **31**, 1338 (1985).
6. R. H. Anderson and M. Miller, *Phys. Rev. B* **40**, 2109 (1989).
7. E. Krotscheck, G. X. Qian, and W. Kohn, *Phys. Rev. B* **31**, 4245 (1985); (b) E. Krotscheck, M. Saarela, and J. L. Epstein, *Phys. Rev. B* **38**, 111 (1988), and references therein; (c) E. Krotscheck, M. Saarela, and J. L. Epstein, *Phys. Rev. Lett.* **61**, 1728 (1988).
8. F. Dalfovo and S. Stringari, *Physica Scripta* **38**, 204 (1988).
9. N. Pavloff and J. Treiner, *J. Low Temp. Phys.* (in press).
10. V. R. Pandharipande, S. C. Pieper, and R. B. Wiringa, *Phys. Rev. B* **34**, 4571 (1986).
11. S. Stringari and J. Treiner, *Phys. Rev. B* **36**, 8369 (1987).
12. D. O. Edwards and P. P. Fatouros, *Phys. Rev. B* **17**, 2147 (1978).
13. M. Himbert, J. Dupont-Roc, N. Pavloff, and J. Treiner, *J. Low Temp. Phys.* **81**, 31 (1990).
14. P. Tarazona, *Phys. Rev. A* **31**, 2672 (1985), and references therein.
15. R. Cowley and A. D. B. Woods, *Can J. Phys.* **49**, 177 (1971).
16. D. O. Edwards, P. P. Fatouros, G. G. Ihas, P. Mrozinski, S. Y. Shen, F. M. Gasparini, and C. P. Tam, *Phys. Rev. Lett.* **34**, 1153 (1975); U. Nayak, D. O. Edwards, and N. Masuhara, *Phys. Rev. Lett.* **50**, 990 (1983).
17. N. Pavloff and J. Treiner, in preparation.
18. F. Dalfovo and S. Stringari, *Phys. Lett. A* **112**, 171 (1985).
19. J. Epstein, E. Krotscheck, and M. Saarela, *Phys. Rev. Lett.* **64**, 427 (1990).
20. H. J. Lauter, H. P. Schildberg, H. Godfrin, H. Wiechert, and R. Haensel, *Can. J. Phys.* **65**, 1435 (1987), and references therein.
21. R. H. Higley, D. T. Sprague, and R. B. Hallock, *Phys. Rev. B* (submitted).
22. X. Wang and F. M. Gasparini, *Phys. Rev. B* **38**, 11245 (1988).
23. J. C. Noiray, D. Sornette, J. P. Romagnan, and J. P. Laheurte, *Phys. Rev. Lett.* **53**, 2421 (1984); J. P. Laheurte, J. C. Noiray, J. P. Romagnan, and D. Sornette, *J. Phys.* (Paris) **47**, 39 (1986).
24. R. B. Hallock, *Can. J. Phys.* **65**, 1517 (1987).
25. B. Statt, private communication.